Title:

Mitigating nitrous oxide emission by an ultra-fast bioprocess enabling the removal of high concentration N_2O

Authors:

Ryota Maeda[1], Mikiko Sato[1], Kiwamu Minamisawa[2] and Kengo Kubota[1,3,*]

Affiliations:

[1] Department of Frontier Sciences for Advanced Environment, Graduate School of Environmental Studies, Tohoku University, 6-6-06 Aza-Aoba, Aramaki, Aoba-ku, Sendai, Miyagi 980-8579, Japan

[2] Department of Ecological Developmental Adaptability Life Sciences, Graduate School of Life Science, Tohoku University, 2-1-1 Katahira, Aoba-ku, Sendai, 980-8577, Japan

[3] Department of Civil and Environmental Engineering, Graduate School of Engineering, Tohoku University, 6-6-06 Aza-Aoba, Aramaki, Aoba-ku, Sendai, Miyagi 980-8579, Japan

Corresponding Author:

*Kengo Kubota

Department of Frontier Sciences for Advanced Environment, Graduate School of Environmental Studies, Tohoku University, 6-6-06 Aoba, Aramaki, Aoba-ku, Sendai, Miyagi 980-8579, Japan.

Tel. & Fax: +81-22-795-5011

E-mail: kengo.kubota.a7@tohoku.ac.jp

Abstract

Nitrous oxide (N_2O) is known as a greenhouse gas as well as an ozone-depleting substance. Wastewater treatment process is one of the sources of N_2O emission, and the high concentrations of N_2O in off-gas were reported from an anaerobic ammonium oxidation process. This study developed a novel N_2O removal process using a down-flow hanging sponge reactor to remove high concentrations of N_2O. More than 96% removal efficiencies were achieved for up to 300 ppm N_2O with 3 min gas retention time (GRT), and more than 99% removal efficiency was obtained for 2,000 ppm N_2O with 18 min GRT. A maximum removal rate of 161 ± 26 mg-N/L-reactor/day was achieved, that was over 10 times faster than the pioneering process. Kinetic analysis indicated that the N_2O dissolution rate is a crucial factor in determining the N_2O removal rate in the reactor. Various N_2O reducers belonging to both clade I and II were detected in reactors, and *Azonexus* was thought to play a key role.

Keywords:

Down-flow hanging sponge (DHS); kinetics; metagenome; microelectrode; nitrous oxide (N_2O); *nosZ* gene; 16S rRNA gene amplicon

1. Introduction

Nitrous oxide (N_2O) is a greenhouse gas and an ozone-depleting substance (Ravishankara et al., 2009). Its atmospheric concentration has increased significantly over the last 100 years, reaching 336 ppb in 2022 (IPCC, 2022; Tian et al., 2020). N_2O has approximately 273 times greater global warming potential than that CO_2 and has a lifetime of 114 years in the atmosphere. The recent increase in N_2O emissions exceeds the worst-emission scenario of the IPCC; therefore, the reduction of N_2O emissions is an urgent issue globally (Tian et al., 2020). The agricultural sector is the main source of N_2O emissions, accounting for more than half of human activity-related emissions. Although their contribution is much lower, the waste and wastewater treatment sectors are also sources of N_2O.

In wastewater treatment, N_2O is generated in both aerobic and anaerobic processes related to nitrogen removal (i.e. nitrification and denitrification) by biotic and abiotic transformation processes (e.g. nitrifier denitrification, hydroxylamine oxidation, and incomplete denitrification) (Hallin et al., 2018; Sabba et al., 2018). Earlier studies identified several factors that influence N_2O generation from wastewater treatment processes (e.g. dissolved oxygen (DO), nitrite and ammonium concentrations, and the chemical oxygen demand (COD) /N ratio) (Domingo-Félez and Smets, 2019; Kampschreur et al. 2009; Vasilaki et al. 2019; Wu et al. 2020). N_2O emission mitigation approaches, such as DO

control (Duan et al., 2021) and COD/N ratio control through carbon source input (Hu et al., 2013; Peng et al., 2017) were reported. However, these approaches are not necessarily universal because they are only effective under specific conditions (Han et al., 2023; Oba et al., 2024). As an alternative approach, processes removing N_2O in off-gas using microbial reactions were developed (e.g., utilising a fixed bed reactor packed with Kaldnes rings (Frutos et al., 2016) or biofilters filled with polyurethane foam (Han et al., 2023; Yoon et al., 2019, 2017)). These studies targeted 100–300 ppm of N_2O in either N_2 (anaerobic) or air (aerobic) and successfully reduced N_2O in the gaseous phase.

In addition to conventional nitrification-denitrification processes, anaerobic ammonium oxidation (anammox) is being considered for the removal of nitrogen from wastewater. More than 100 anammox-based full-scale plants are used globally to treat industrial and municipal wastewater (Lackner et al., 2014). The generation of N_2O from anoxic anammox tanks were reported (Ali et al., 2016; Kampschreur et al., 2009, 2008; Okabe et al., 2011; Vasilaki et al., 2019) with concentrations reaching 1,300 ppm (laboratory-scale) (Okabe et al., 2011) and 4,000 ppm (full-scale) (Kampschreur et al., 2008) in off-gas, which is much higher than that of the previously tested concentrations for N_2O removal (200 ppm in N_2) (Yoon et al., 2017).

To remove high concentrations of N_2O generated from anaerobic/anoxic wastewater treatment processes, such as anammox processes, we focused on down-flow hanging sponge

81 (DHS) processes. DHS was originally developed for wastewater treatment, maintaining high
82 sludge biomass in sponge media and resulting in effluent water quality comparable to that of
83 conventional activated sludge processes. It allows aerobic treatment without aeration by
84 supplying oxygen from the air due to gas-liquid equilibrium, while wastewater flows from top
85 to bottom due to gravity (Kubota et al., 2024). The application of DHS reactors for gaseous
86 substances such as hydrogen sulfide and toluene were reported by using the closed reactors
87 (Tanikawa et al., 2022; Yamaguchi et al., 2018).

88 In this study, we developed a process that rapidly removed high concentrations of N_2O
89 using DHS. The N_2O removal performance of the DHS reactors was evaluated by feeding
90 different concentrations of N_2O (5–2,000ppm) and supplying the supernatant from an
91 anaerobic sewage sludge digester as a carbon source. Microelectrode experiments were
92 conducted to assess the kinetics of the N_2O reduction. Eventually, the microorganisms that
93 may be involved in N_2O removal were identified using 16S rRNA gene amplicon and shotgun
94 metagenome analyses.

95

96 **2. Material and Methods**

97 **2.1 Reactor configuration and operation**

98 A DHS reactor consisting of fifteen sponge carriers with polyethene plastic net rings was
99 placed in a closed column with a volume of 1.23 L. The carriers were vertically connected

100 and suspended in the column. The size of polyurethane sponge was 30 mm in diameter and 30

101 mm in height. The total sponge volume was 0.32 L, resulting in a packing density of 26%.

102 Anaerobic sludge obtained from an anaerobic digester treating sewage sludge under

103 mesophilic conditions was used as the seed sludge. The supernatant of the digested sludge

104 was used as a carbon source and fed from the top of the reactor with a hydraulic retention

105 time (HRT) of 3–24 hours based on the sponge volume. Feeding was performed intermittently

106 using a timer. N_2 gas containing 5, 40, 300 or 2,000 ppm N_2O was subjected to the closed

107 column from the inlet near the bottom of the reactor. The outlet for the treated gas was placed

108 near the top of the reactor, resulting in gas flow from the bottom to the top. The gas flow rate

109 was adjusted using a gas meter (RK1200; KOFLOC, Kyoto, Japan). The gas retention time

110 (GRT) was adjusted by varying the gas flow rate. The reactor was set in an incubation

111 chamber and operated anaerobically at 25ºC in the dark. The GRT was calculated by using a

112 gas volume at 25ºC and an effective reaction volume of 0.91 L. Nitrogen loading of the

113 reactor was calculated by using a reactor volume of 1.23 L and the amount of nitrogen under

114 the standard temperature (0ºC). A schematic of the experiment is shown in Fig.1.

115

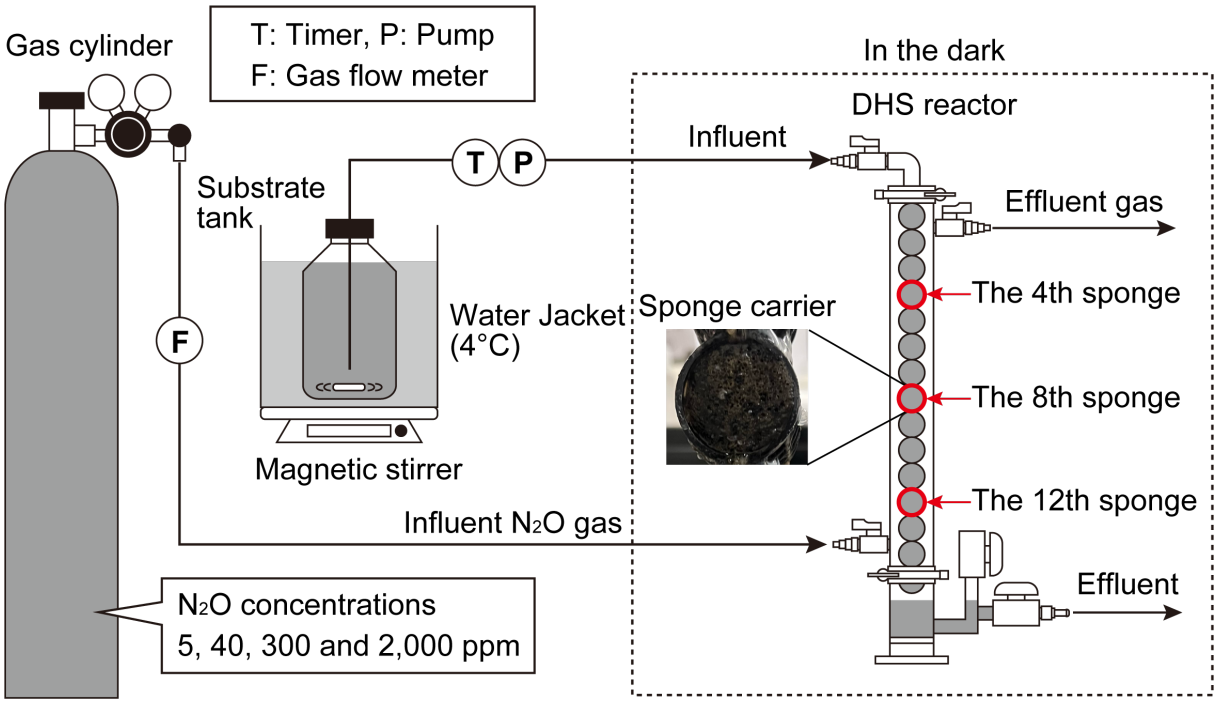

Fig. 1. Schematic diagram of the experiment. The sludge samples collected from the 4th, 8th and 12th sponges from the top were used for the microelectrode experiments. The 4th and 12th sponges were used for 16S rRNA amplicon and metagenome analyses.

2.2 Measurement of gaseous N_2O concentration

The effluent gas from the closed DHS reactor was measured every 1–2 days to evaluate N_2O removal performance. In this study, two sets of electron capture detector gas chromatography (ECD-GC) (GC-2014, Shimadzu, Kyoto, Japan) with different columns were used, depending on the N_2O concentration. Both ECD-GCs were equipped with a 63Ni ECD, and N_2 was used as the carrier gas. For the measurement of lower N_2O concentrations (< approximately 40 ppm), an ECD-GC with a tandem Porapak Q column (80/100 mesh; 3.0 mm × 1.0 m and 3.0 mm × 2.0 m, GL Sciences, Japan) was used. The temperatures were set at

129 80°C, 100°C, and 340°C for the column, injector, and detector, respectively. For the
130 measurement of higher N_2O concentrations (> approximately 40 ppm), an ECD-GC with a
131 TC-BOND Q column (0.53 mm × 30 m, df=20 μm, GL Sciences, Japan) was used. The
132 temperatures were set at 50°C, 280°C, and 300°C for the column, injector, and detector,
133 respectively.
134
135 **2.3 Water quality analysis and sludge sampling**
136 Influent water and effluent water from the DHS reactor were sampled to evaluate
137 changes in water quality. COD was measured using a HACH water quality analyser (DR890,
138 HACH, Loveland, CO, USA).
139 Sludge samples were collected on the final experimental day. A sponge was immersed
140 in 0.05 × phosphate buffered saline (PBS; 130 mM NaCl, 10.8 mM Na_2HPO_4, 4.2 mM
141 NaH_2PO_4, pH 7.4) in a plastic bag, and sludge was suspended in PBS by squeezing the
142 sponges. Part of the suspended sludge was used for microelectrode experiments (see Section
143 2.4). The other part was centrifuged at 2935×g for 15 min at 4°C. After removing the
144 supernatant, a portion of the sludge was stored at -20°C for DNA extraction. The other part
145 was used to measure the suspended solids (SS) and volatile suspended solids (VSS) according
146 to the standard methods (APHA, 2017).
147

148 **2.4 Microelectrode experiment for measuring N_2O consumption rate**

149 The N_2O consumption rates of the sludge samples were measured using an N_2O
150 micro-respiration system with amperometric microsensors (Unisense, Aarhus, Denmark) (Fig.
151 S1). Measurements and subsequent data analyses were conducted in accordance with an
152 earlier study (Suenaga et al., 2018). Briefly, the sludge samples collected from the 4th, 8th
153 and 12th sponges (Fig. 1) were used for the experiments. The sludge samples were initially
154 diluted with anaerobic sludge digester supernatant, which was filter sterilised by using 0.22
155 μm Stericup® filter (S2GVU01RE, Merck Millipore, Germany) to make sludge concentration
156 suitable for the microelectrode experiment. Approximately 8 ml double-port chamber
157 (Unisense, Aarhus, Denmark) was filled with the sample and placed in a water bath controlled
158 at 25°C. N_2O sensors were inserted into the chamber, and a certain amount (30–40 μl) of N_2O
159 water prepared by aerating pure N_2O gas was injected into the chamber using a Hamilton
160 syringe. The sample was stirred at 600 rpm, and the N_2O concentration was continuously
161 recorded using SensorTrace Suite ver. 2.8.0 (Unisense). After the injected N_2O was
162 completely consumed, fresh N_2O water was injected, and N_2O consumption was measured.

163 For the data analysis, noise removal and plot smoothing were performed using Sigma
164 Plot 13.0 (Systat Software, San Jose, CA, USA). The theoretical maximum consumption rate
165 of N_2O (V_{max}) was obtained using the Michaelis-Menten equation and the Excel solver
166 function (Suenaga et al., 2018). The theoretical maximum N_2O removal rate per reactor

167 volume (mg-N/L-reactor/day) was calculated by multiplying V_{max} (N_2O removal rate per

168 VSS) by the amount of VSS in the reactor.

169

170 **2.5 16S rRNA gene amplicon sequence analysis**

171 Sludge samples collected from the 4th and 12th sponges of each reactor were

172 subjected to 16S rRNA gene amplicon sequencing analysis. DNA extraction was performed

173 using ISOIL for Beads Beating kits (Nippon Gene, Tokyo, Japan), according to the

174 manufacturer's instructions. Prokaryotic 16S rRNA genes were amplified using 341f

175 (5'-CCTAYGGGGRBGCASCAG-3') and 806r mix (806r (5'-

176 GGACTACHVGGGGTHTCTAAT-3') and 806r-P (GGACTACCAGGGTATCTAAG-3') in

177 a 30:1 ratio) (Matsubayashi et al., 2017). The PCR conditions for library preparation were as

178 described earlier (Ni et al., 2020). 16S rRNA gene amplicon sequencing using the MiSeq

179 Reagent Kit v3 600 cycles was outsourced to the Bioengineering Lab. Co., Ltd. (Kanagawa,

180 Japan). Nucleotide sequence data are available in the DDBJ Sequence Read Archive

181 accession number PRJDB18886.

182 Data analysis was conducted using QIIME2 ver. 2023.7 (Bolyen et al., 2019).

183 Quality trimming, primer sequence removal, paired-end assembly, and chimaera checking of

184 the raw 16S rRNA gene sequencing data were performed using DADA2 (Callahan et al.,

185 2016). The 16S rRNA gene sequences with ≥ 97% identity were clustered into operational

186 taxonomic units (OTUs) using VSEAECH (Rognes et al., 2016). The OTUs were classified
187 using the Greengens2 database (McDonald et al., 2023).
188
189 **2.6 Shotgun metagenome analysis**
190 DNA extracted from the 4th and 12th sponges in each reactor was subjected to
191 short-read metagenomic analysis. Library preparation and sequencing were outsourced to the
192 Bioengineering Lab. Co., Ltd.. In brief, sequencing libraries were prepared using the
193 MGIEasy FS DNA Library Prep Set (MGI Tech, Shenzhen, China) and 150 bp paired-end
194 reads were generated using DNBSEQ-G400 (MGI Tech). Nucleotide sequence data are
195 available in the DDBJ Sequence Read Archive accession number PRJDB18886.
196 The generated reads were subjected to SOAPnuke 2.0.6 (Chen et al., 2018) to
197 remove the adaptor sequences and low-quality reads. Assembly was performed using the
198 workflow “aviary assemble” in Aviary 0.8.3 (Newell et al., 2023). Contigs shorter than 600
199 bp were excluded from subsequent analyses. Contigs containing putative *nosZ* gene sequences
200 were retrieved using the BLASTN algorithm (Altschul et al., 1990) and a *nosZ* database
201 (Zheng et al., 2023). The coverage of contigs was analysed coverM 0.7.0 (Aroney et al.,
202 2024), and the relative abundance of each *nosZ* gene was calculated. The obtained contigs
203 were subjected to the workflow "aviary annotate" and Prokka 1.14.6 (Seemann, 2014) for

204 functional annotation. Eventually, contigs containing NosZ protein sequences with ≥ 300
205 amino acids were extracted to construct a phylogenetic tree.
206 A phylogenetic tree of the NosZ sequences obtained in this study was constructed using
207 known reference NosZ sequences. The reference sequences were obtained by clustering the
208 *nosZ* gene sequences (Zheng et al., 2023) with 70% sequence identity using VSEARCH
209 2.27.0. The reference sequences (n=574) were converted to amino acid sequences. The amino
210 acid sequences were aligned using MAFFT (Katoh et al., 2002) and trimmed using TrimAl
211 (Capella-Gutiérrez et al., 2009). A phylogenetic tree was constructed using IQ-tree2 (Minh et
212 al., 2020). The best-fit model was LG + F + R10, as determined using ModelFinder
213 (Kalyaanamoorthy et al., 2017). The phylogenetic tree was visualised using iTOL v6 (Letunic
214 and Bork, 2021).
215
216 **3. Results**
217 **3.1 N_2O removal performance by DHS reactors**
218 In this study, the continuous treatment of gaseous N_2O was conducted using DHS
219 reactors. The N_2O removal performance was evaluated using different concentrations of N_2O
220 in N_2 (5, 40, 300 and 2,000 ppm) under various N_2O loads by changing the gas flow rates
221 (shortest GRT of 3 min) (Fig. 2 and Tables S1 and S2). Hereafter, each reactor is denoted as 5,
222 40, 300, and 2,000 ppm N_2O reactor.

223 The 5 ppm N_2O reactor (Fig. 2a and Table S1) started with a GRT of 18 min. The N_2O
224 removal efficiency reached over 90% after one day, and high removal performance was kept
225 even at a GRT of 9.1 and 4.6 min. Finally, the removal efficiency of 97 ± 5.4% was obtained
226 under the GRT of 3.0 min with the N_2O removal rate of 2.0 ± 0.1 mg-N/L-reactor/day.
227 The 40 ppm N_2O reactor (Fig. 2b, Table S1) also showed high removal efficiency after
228 starting up, showing 95 ± 3.9% and 99 ± 0.9% removal efficiency under the GRT of 18 min
229 and 9.1 min by day 20, respectively. When the GRT was shortened to 6.1 min, the removal
230 efficiency dropped to 74 ± 17% (days 20–50) due to insufficient COD supply (Fig. 2b and
231 Tables S1 & S2). After supplying sufficient COD, N_2O removal became stable with the
232 removal efficiency of 96 ± 3.4% under the GRT of 3.6 min (days 71–85, removal rate; 13 ±
233 0.5 mg-N/L-reactor/day).
234 The N_2O removal performance of the 300 ppm N_2O reactor (Fig. 2c and Table S1) was
235 similar to the 40 ppm N_2O reactor. Over 99% removal efficiency was obtained under the GRT
236 as short as 6.1 min (days 61–70), except for the term of days 20–50, during which the COD
237 supply was deficient, and the removal efficiency dropped to 39 ± 16%. On day 70, reactor
238 operation was stopped for unavoidable reasons (Fig. 2c). After a few weeks of suspension, the
239 reactor was restarted with new sponges and seed sludge by feeding 300 ppm N_2O gas with a
240 GRT of 6.1 min (the day of re-start-up was set as day 71 for convenience). An N_2O removal
241 rate of over 97% was achieved after four days of operation. The GRT was further shortened to

3.0 min, resulting in the N_2O removal efficiency of 94 ± 1.5% (days 108–117, removal rate; 113 ± 1.8 mg-N/L-reactor/day).

The 2,000 ppm N_2O reactor (Fig. 2d and Table S1) was initially operated at a GRT of 18 min. The removal efficiency in the first week was only 57 ± 1.5%; therefore, the GRT was extended to 36 min, resulting in the removal efficiency of 98 ± 6.7%. The GRT was set at 18 min again, and low removal efficiency of 36 ± 18% was observed because of insufficient COD supply (days 20–50) (Fig. 2d and Tables S1 and S2). High removal efficiency of 99 ± 0.6% was achieved with increased organic loading rate (days 61–70). The reactor was stopped after 70 days of operation. Similar to the 300 ppm N_2O reactor, new seed sludge was inoculated, and the reactor was restarted with a GRT of 18 min. The removal efficiency reached ≥ 99% again after 12 days of operation, and the stable and high removal efficiency of 99 ± 0.1% was observed on days 83–86 (removal rate; 132 ± 0.1 mg-N/L-reactor/day) (Fig. 2d and Table S1). High removal efficiency was not achieved even under higher organic loading rate at the GRT of 9.1 min. Lower N_2O removal efficiency of 61 ± 10% was obtained (days 87–119), but the highest N_2O removal rate of 161 ± 26 mg-N/L-reactor/day was achieved in this period.

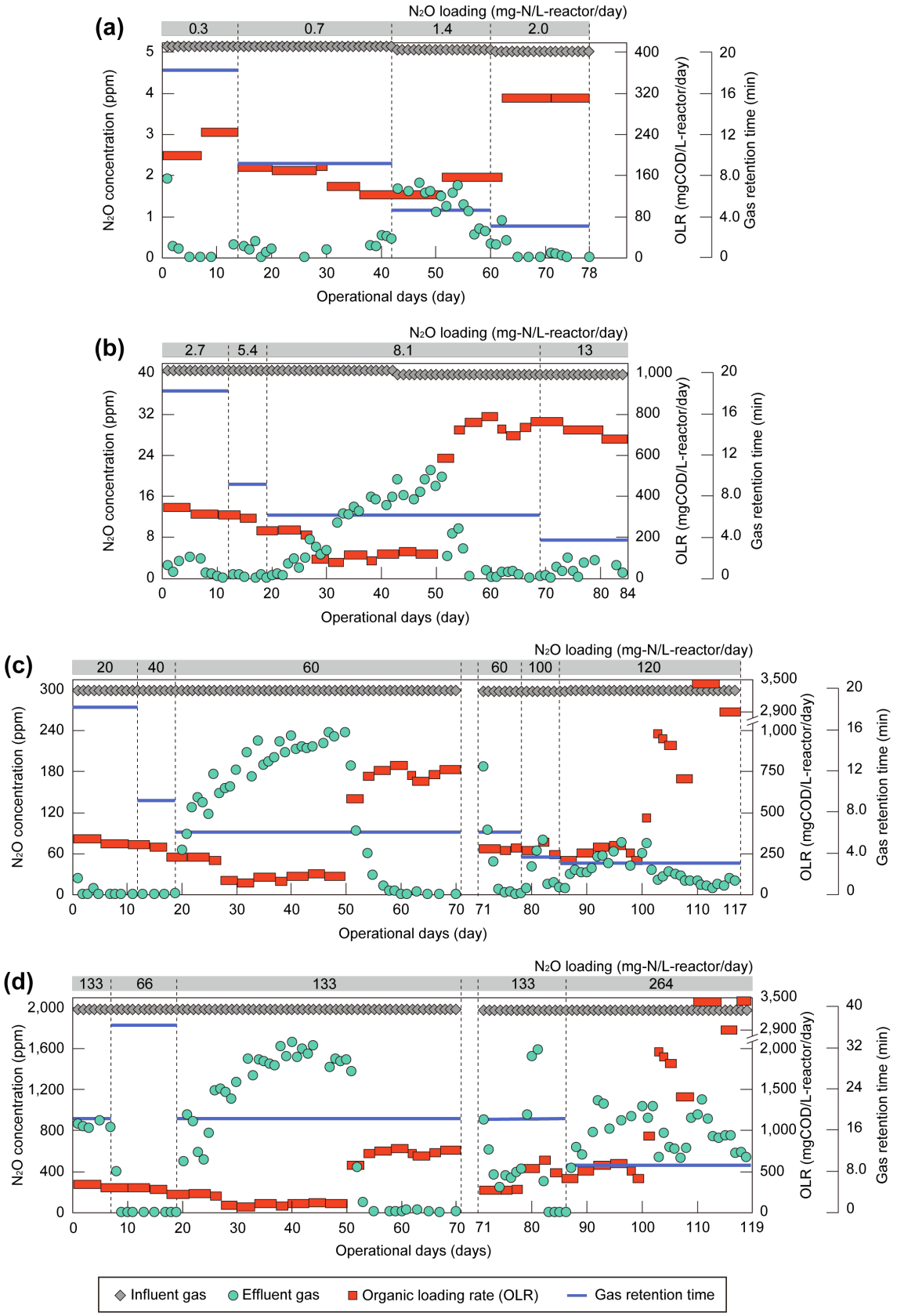
(a)
N2O loading (mg-N/L-reactor/day)
0.3
0.7
1.4
2.0
N2O concentration (ppm)
OLR (mgCOD/L-reactor/day)
Gas retention time (min)
Operational days (day)
(b)
N2O loading (mg-N/L-reactor/day)
2.7
5.4
8.1
13
N2O concentration (ppm)
OLR (mgCOD/L-reactor/day)
Gas retention time (min)
Operational days (day)
(c)
N2O loading (mg-N/L-reactor/day)
20
40
60
60
100
120
N2O concentration (ppm)
OLR (mgCOD/L-reactor/day)
Gas retention time (min)
Operational days (day)
(d)
N2O loading (mg-N/L-reactor/day)
133
66
133
133
264
N2O concentration (ppm)
OLR (mgCOD/L-reactor/day)
Gas retention time (min)
Operational days (days)
Influent gas
Effluent gas
Organic loading rate (OLR)
Gas retention time

259

260 Fig. 2. Nitrous oxide (N_2O) removal performance. Different concentrations of N_2O in

261 nitrogen gas were treated under different gas retention times and organic loadings. a; 5 ppm

262 N_2O, b; 40 ppm N_2O, c; 300 ppm N_2O, d; 2,000 ppm N_2O.

263

264 **3.2 N_2O consumption rate**

265 The N_2O consumption rates of the sludge collected from the 300 ppm and 2,000 ppm

266 N_2O reactors were measured using microelectrodes, as described earlier (Suenaga et al. 2018)

267 (Fig. S1). Theoretical maximum N_2O removal rates calculated using the Michaelis-Menten

268 equation were 1,189 ± 257 mg-N/L-reactor/day and 1,468 ± 186 mg-N/L-reactor/day at the

269 300 ppm and 2,000 ppm N_2O reactor, respectively (Table 1). Simultaneously, the actual

270 highest N_2O consumption rates of the reactors were 113 ± 1.8 mg-N/L-reactor/day (days

271 108–117 for the 300 ppm N_2O reactor) and 161 ± 26 mg-N/L-reactor/day (days 102–119 for

272 the 2,000 ppm N_2O reactor). These values were approximately 10% of the theoretical

273 maximum N_2O consumption rate.

274

275

276

277

278

279 Table 1. Nitrous oxide removal rates.

Reactor	Maximum N_2O removal rate of the reactor (mg-N/L-reactor/day)	The calculated theoretical N_2O removal rate (based on the Michaelis–Menten equation) (mg-N/L-reactor/day) [a]
300 ppm N_2O	113 ± 1.8 (days 108–117)	1,189 ± 257
2,000 ppm N_2O	161 ± 26 (days 102–119)	1,468 ± 186

280 [a] N_2O removal rate per reactor volume was calculated based on the amount of volatile

281 suspended solids retained in the reactor.

282

283 **3.3 Microbial community involved in N_2O reduction**

284 **3.3.1 16S rRNA gene amplicon analysis**

285 The microbial communities of the sludge samples evaluated by 16S rRNA gene

286 amplicon analysis are shown in Table S3, and the top 30 OTUs with average relative

287 abundances are summarised in Fig. 3. The microbial communities built in the reactors

288 differed from those in the seed sludge and substrate, as demonstrated by principal coordinate

289 analysis (PCoA) (Fig. S2). The microbial community structures changed with N_2O

290 concentrations and along the height of the reactors, although the N_2O concentrations had the

291 greatest effect.

292 Some OTUs with high relative abundance were similar to known N_2O-reducing

293 microorganisms (Fig. 3). OTU0001, which is close to *Azonexus*_595978, was the most

294 abundant member in all reactors. *Azonexus* is found in partial-denitrification-anammox

295 processes and anaerobic manure digestate and is expected to be involved in N_2O reduction
296 (Huang et al., 2024; Wang et al., 2023). In addition to *Azonexus*, several OTUs close to
297 known N_2O reducers were identified, including *Giesbergeria* (OTU0020) (Zhang et al., 2022),
298 *Thauera*_A_597130 (OTU0013) (Huang et al., 2024), *Denitrificimonas* (OTU0029) (Wang et
299 al., 2024), *Oblitimonas* (OTU0019) (Ramírez-Fernández et al., 2021), and *Sulfurivermis*
300 (OTU0010) (Liu et al., 2023). OTU0020 and OTU0029 were found in reactors with lower
301 N_2O concentrations of 5 and 40 ppm, respectively, whereas OTU0019 was found in reactors
302 with higher N_2O concentrations of 300 ppm and 2,000 ppm. OTU0010 was dominant only in
303 the 2,000 ppm N_2O reactor. Thus, the known N_2O-reducing microorganisms were enriched in
304 the DHS reactors with various concentrations of N_2O.
305 In addition to OTUs close to known N_2O reducers, the relative abundances of many
306 OTUs increased after feeding with N_2O. Although they are not close relatives of N_2O
307 reducers at the genus level, some OTUs belong to the same family as N_2O reducers (e.g.
308 OTU0005 and OTU0009) (Isokpehi et al., 2024). The OTUs increasing the relative
309 abundance could potentially reduce N_2O, although this was difficult to demonstrate using
310 only 16S rRNA gene amplicon analysis.
311

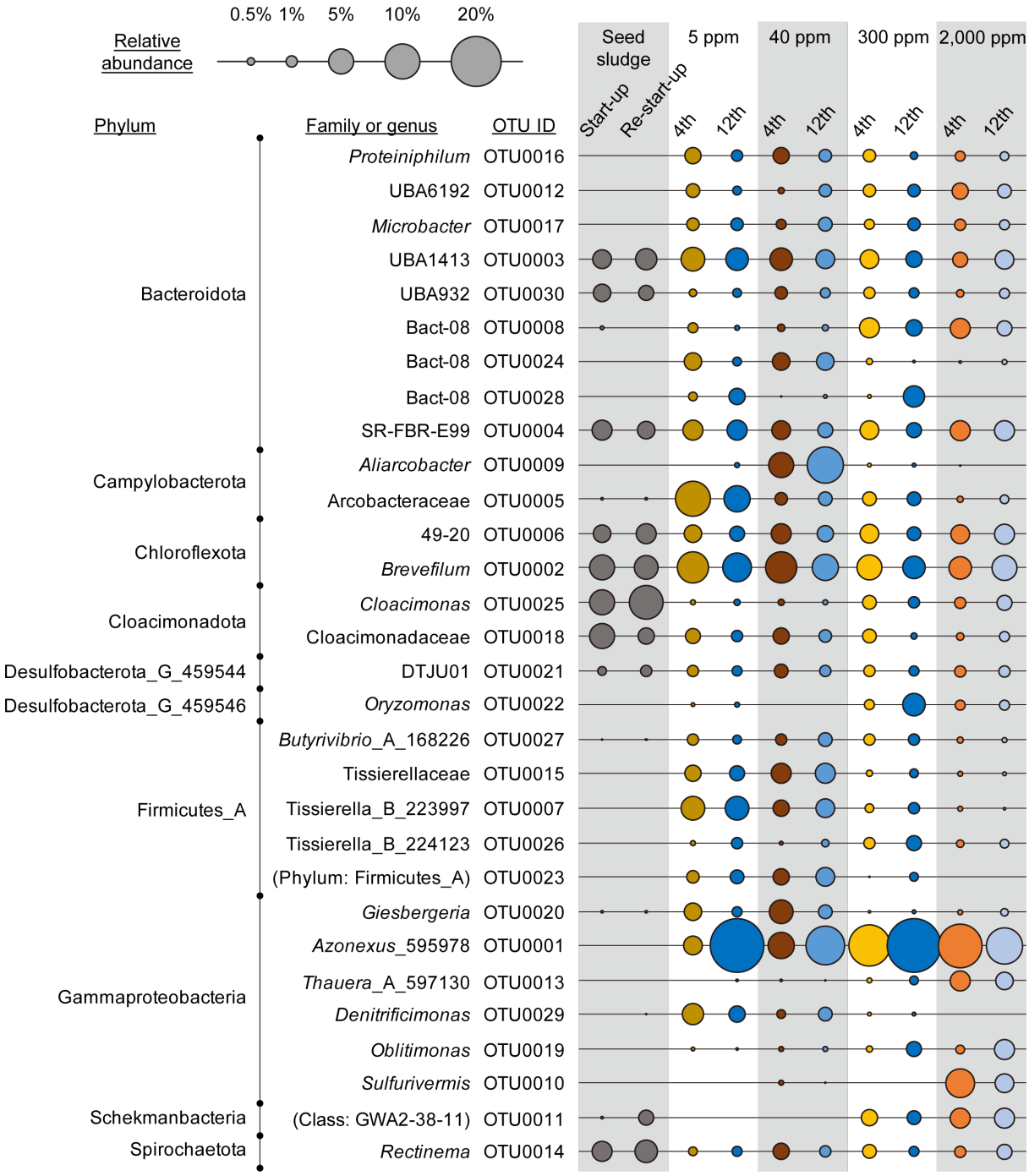

Fig. 3. Top 30 OTUs in the average relative abundance. The size of the circle indicates the relative abundance of OTUs in each sample. 4th: the 4th sponge, 12th: the 12th sponge. Seed sludge: sludge from a mesophilic anaerobic sewage sludge digester.

3.3.2 Metagenome analysis of *nosZ* gene

318 In total, 229 contigs, including a sequence homologous to *nosZ*, were obtained (matched
319 by BLASTN with sequences longer than approximately 600 bp) (Table S4). The phylogenetic
320 tree of *nosZ* extracted from metagenomic 229 contigs (Fig. 4) revealed that clade II *nosZ* gene
321 was more diverse and abundant than clade I *nosZ* gene in the reactors. The most abundant
322 *nosZ* genes retrieved from all reactors were similar to those in *Azonexus*, harboring clade II
323 *nosZ* gene. In the 2,000 ppm N_2O reactor, other than *Azonexus nosZ* gene,
324 *Sulfurivermis*-related *nosZ* gene was obtained in high abundance. This *nosZ* gene was not
325 detected in the other reactors. Additionally, the *Aliarcobacter*-related *nosZ* gene was only
326 found in the 40 ppm N_2O reactor, which was identical to the amplicon analysis (i.e.
327 OTU0009). Besides these microorganisms, *nosZ* gene-harboring microorganisms detected in
328 both 16S rRNA gene amplicons and metagenomic analyses were *Giesbergeria* and *Thauera*,
329 both harboring clade I *nosZ* gene.
330

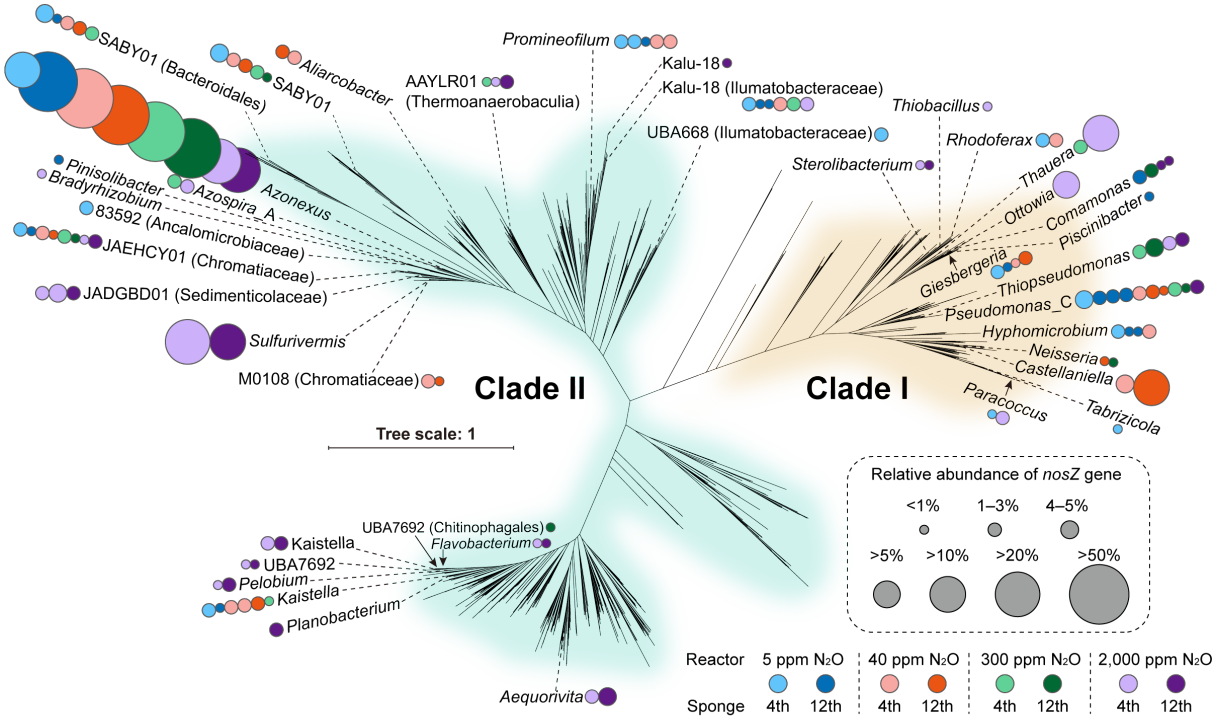

Fig. 4. Phylogenetic tree of NosZ protein. The size of the circles indicates the relative abundance of read counts of contigs with the *nosZ* gene. The colours represent the nitrous oxide concentrations fed to the reactors. 4th: the 4th sponge, 12th: the 12th sponge.

4. Discussion

4.1 Ultra-fast bioprocess for mitigating high concentration N_2O emission

This study demonstrated that the DHS is able to remove N_2O in N_2 gas with removal efficiencies of over 96% for concentrations of up to 300 ppm at 3 min GRT and 2,000 ppm at 18 min GRT with the supply of real wastewater, i.e., the supernatant of sewage sludge digestate. The highest removal rate of 161 ± 26 mg-N/L-reactor/day was achieved when 2,000 ppm N_2O was supplied with a GRT of 9.1 min. One study investigated the removal of N_2O in

343 N_2 gas using a biofilter reactor packed with 2 cm × 2 cm × 2 cm polyurethane cubes (Yoon et
344 al., 2017). This study achieved a removal efficiency of ≥ 99% for 200 ppm N_2O in N_2 gas at
345 GRT of 8.9 min with synthetic wastewater and a removal efficiency of 80–90% at GRT of
346 32.2 min with wastewater from a primary sedimentation basin treating sewage. Our study
347 demonstrated a much faster treatment (over 10 times) capable of removing higher
348 concentrations of N_2O in N_2 gas compared to that of a previous study, even with the use of
349 real wastewater.

350 High concentrations of N_2O in off-gas were reported, especially from anammox
351 processes, e.g. 0.4–240 ppm (Ali et al., 2016) and 93–1,358 ppm (Okabe et al., 2011) from
352 lab-scale reactors and >4,000 ppm (Kampschreur et al., 2008) from a full-scale reactor
353 although the anammox reaction itself is thought not to produce N_2O (Harris et al., 2015;
354 Kartal et al., 2007). Although the highest concentration tested in this study (i.e., 2,000 ppm)
355 was lower than 4,000 ppm, it showed the potential to remove such high concentrations of N_2O
356 from nitrogen gas. A longer GRT is most probably needed, although a higher removal
357 efficiency can be achieved with a sufficient supply of electron donors, which is directly
358 related to the removal efficiencies of the reactor, as shown in Fig. 2bcd (days 20–50 for the 40,
359 300 and 2,000 ppm reactors).

360 To minimise the amount of N_2O emission from wastewater treatment processes, research
361 focusing solely on N_2O removal efficiency can be misleading. In this study, a removal

362 efficiency of approximately 99% was achieved with a GRT of 18 minutes when 2,000 ppm of

363 N_2O was supplied. However, approximately 20 ppm of N_2O still remained in the off-gas.

364 Particularly in cases where high concentrations of N_2O are treated, implementing an

365 additional treatment process for N_2O removal from the off-gas can further minimise the final

366 N_2O emissions from the process (e.g., a series of DHS reactors).

367

368 **4.2 Kinetics of N_2O reduction in bioreactor**

369 Microelectrode experiments showed an approximately 10-fold faster kinetic potential

370 (Table 1). This suggests that the microbial community inhabiting the reactor had a much

371 greater capacity to reduce N_2O to N_2. Dissolved N_2O was supplied directly to the stirred

372 sludge during the microelectrode experiments (Fig. S1). On the other hand, in the reactor,

373 gaseous N_2O needs to be initially dissolved in the liquid, and then microorganisms can utilise

374 the dissolved N_2O. Thus, the N_2O dissolution rate is the key to determine the removal rate in

375 the reactor.

376 The dissolution rate from gas to liquid can be explained using the Nernst-Noyes-Whitney

377 equation (Dokoumetzidis and Macheras, 2006; Noyes and Whitney, 1897). In the

378 Nernst-Noyes-Whitney equation, the dissolution rate constant (given by the diffusion

379 coefficient of the substance, volume of the solution, and thickness of the diffusion layer),

380 surface area, concentration of the dissolved substance at a given time t, and saturation

381 solubility of the substance were considered. Without N_2O consumption in the liquid phase,
382 the dissolution rate decreases as N_2O dissolves and eventually reaches equilibrium, at which
383 point no more N_2O is removed from the gas phase. However, when microorganisms are
384 present in the liquid phase and actively consume N_2O, the N_2O concentration in the liquid
385 remains low, and the diffusion layer becomes thinner, allowing the dissolution rate to remain
386 high.

387 To achieve faster dissolution rates, it is suggested to increase the surface area of the
388 carrier or enhance the microbial activity near the sponge surface to decrease the dissolved
389 N_2O concentration and reduce the thickness of the diffusion layer. One could consider
390 supplying different substrates utilised by other microorganisms to enhance microbial activity
391 to enable faster N_2O reduction. An earlier study (Yoon et al., 2017) reported a higher N_2O
392 removal efficiency with synthetic wastewater than that with real wastewater, i.e., effluent
393 from a primary sedimentation basin treating sewage. Additionally, increasing the temperature
394 would help accelerate the microbial N_2O reduction rate and increase the diffusion coefficient;
395 however, it also causes the decrease of saturation solubility of N_2O. Decreasing the
396 temperature might help elevate dissolution rates by increasing the saturation solubility of N_2O
397 although decreased microbial N_2O reduction rates are expected.

398

399 **4.3 Nitrous oxide reducers in bioreactors**

400 Sludge from the sponges in each reactor was collected on the last day of operation and
401 subjected to 16S rRNA amplicon sequencing analysis. A comparison of the microbial
402 community structure based on PCoA (Fig. S2) showed that the microbial communities in the
403 N_2O-reducing DHS reactors were different from those in the seed sludge, i.e., sludge from an
404 anaerobic sewage sludge digester, as well as those in the supernatant of an anaerobic sludge
405 digestate, i.e., the substrate for denitrification. It also showed a change in the microbial
406 community under different N_2O concentrations, as well as in the height of the reactor (Figs. 3
407 and S2). In a DHS reactor, COD load changes along the height (Kubota et al., 2014), i.e.,
408 higher and lower COD concentrations occur in the upper and lower part of the reactor,
409 respectively. Additionally, the supernatant of the anaerobic sludge digestate contains diverse
410 electron donors. These characteristics provide a habitat for a variety of microorganisms in the
411 reactors compared with that of earlier studies using a simple substrate for N_2O reduction (e.g.,
412 acetate for Conthe et al. 2018).
413 In the N_2O reducing DHS reactors, *Azonexus* was the most abundant genus after both
414 amplicon and metagenome analyses (Fig. 3 and Table S4). *Azonexus* can utilise intermediates
415 of anaerobic organic degradation such as acetate and propionate (Quan et al., 2006). The
416 digestate supernatant contained a small number of fatty acids. Additionally, the substrate may
417 be anaerobically degraded in the reactor, and the intermediates may be used by *Azonexus* as
418 carbon sources to reduce N_2O. An earlier study detected *Azonexus* in a bioreactor

419 continuously supplying N_2O and acetate under anaerobic conditions (Conthe et al., 2018).

420 Thus, *Azonexus* plays a key role in N_2O removal.

421 Other than *Azonexus*, *Sulfurivermis*, which can also utilise acetate and propionate for

422 nitrate reduction (Watanabe et al., 2019), was found to be the second most abundant

423 denitrifier, with high relative abundance (26% in the 4th sponge and 17% in the 12th sponge)

424 in the 2,000 ppm reactor. Additionally, *Aliarcobacter* was found in the 40 ppm N_2O reactor.

425 Because a slightly larger sponge medium (30 mm in diameter and 30 mm in height) was used,

426 a gradient of dissolved N_2O concentration occurred in the sponge media, which may have

427 involved a variety of microorganisms in N_2O reduction.

428 Both clade I and clade II *nosZ* genes were retrieved from the reactors, but clade II *nosZ*

429 was more predominant and diverse than clade I *nosZ* (Fig. 4). *Azonexus*, the most abundant

430 and a key N_2O reducer of this study, belongs clade II. Generally, microorganisms that possess

431 the clade II *nosZ* gene have lower half-saturation constant (K_m) values and higher affinity than

432 clade I N_2O-reducing microorganisms and are more abundant in environments where low

433 concentrations of N_2O are available (Suenaga et al., 2018; Yoon et al., 2016). However, clade

434 II N_2O-reducers shows higher N_2O consumption rate than clade I N_2O-reducers with some

435 specific carbon sources such as acetate and succinate (Qi et al., 2022), suggesting that limited

436 availability of carbon sources derived from the substrate, i.e., the supernatant of anaerobic

437 sludge digestate, caused the predominance of clade II N_2O-reducers over clade I

438 N_2O-reducers even under the high concentration of N_2O.

439

440 **5. Conclusion**

441 In this study, a novel ultra-fast N_2O removal process using a DHS reactor was

442 developed to remove high concentrations of N_2O generated from anaerobic/anoxic wastewater

443 treatment processes such as an anammox process. Continuous experiments revealed that more

444 than 96% removal rates were achieved for up to 300 ppm N_2O gas with 3 min GRT and 2,000

445 ppm N_2O with 18 min GRT. The maximum N_2O removal rate of 161 ± 26

446 mg-N/L-reactor/day was obtained when 2,000 ppm N_2O was supplied with the GRT of 9.1

447 min, which is over 10 times faster than the pioneering process. Additionally, the lack of

448 organic supply immediately deteriorates the N_2O removal performance. Kinetic analysis

449 indicated that the N_2O dissolution rate is a crucial factor in determining the N_2O removal rate

450 in the reactor. Amplicon and metagenome analyses showed that *Azonexus* played a key role in

451 N_2O removal. A gradient of dissolved N_2O concentration may occur in the sponge carriers,

452 resulting in the involvement of various microorganisms in N_2O reduction.

453

454 **Acknowledgements**

This study was supported by KAKENHI grants (JP19KK0371, JP21H01460) from the Japan Society for the Promotion of Science (JSPS), the Moonshot project JPNP18016, commissioned by the New Energy and Industrial Technology Development Organization (NEDO) and the MEXT WISE Program for Sustainability in Dynamic Earth (SyDE), Japan. RM was supported by a Grant-in-Aid for JSPS Fellows (JP24KJ0429).

References

Ali, M., Rathnayake, R.M.L.D., Zhang, L., Ishii, S., Kindaichi, T., Satoh, H., Toyoda, S., Yoshida, N., Okabe, S., 2016. Source identification of nitrous oxide emission pathways from a single-stage nitritation-anammox granular reactor. Water Res. 102, 147–157. https://doi.org/10.1016/j.watres.2016.06.034

Altschul, S.F., Gish, W., Miller, W., Myers, E.W., Lipman, D.J., 1990. Basic Local Alignment Search Tool. J. Mol. Biol. 215, 403–410.

APHP, 2017. Standard methods for the examination of water and wastewater, 23rd ed, American Public Health Association,Washington DC.

Aroney, S.T.N., Newell, R.J.P., Nissen, J., Camargo, A.P., Tyson, G.W., Woodcroft, B.J., 2024. CoverM: Read coverage calculator for metagenomics (v0.7.0). Zenodo. https://doi.org/10.5281/zenodo.10531254

Bolyen, E., Rideout, J.R., Dillon, M.R., Bokulich, N.A., Abnet, C.C., Al-Ghalith, G.A., Alexander, H., Alm, E.J., Arumugam, M., Asnicar, F., Bai, Y., Bisanz, J.E., Bittinger, K., Brejnrod, A., Brislawn, C.J., Brown, C.T., Callahan, B.J., Caraballo-Rodríguez, A.M., Chase, J., Cope, E.K., Da Silva, R., Diener, C., Dorrestein, P.C., Douglas, G.M., Durall, D.M., Duvallet, C., Edwardson, C.F., Ernst, M., Estaki, M., Fouquier, J., Gauglitz, J.M., Gibbons, S.M., Gibson, D.L., Gonzalez, A., Gorlick, K., Guo, J., Hillmann, B., Holmes, S., Holste, H., Huttenhower, C., Huttley, G.A., Janssen, S., Jarmusch, A.K., Jiang, L., Kaehler, B.D., Kang, K. Bin, Keefe, C.R., Keim, P., Kelley, S.T., Knights, D., Koester, I., Kosciolek, T., Kreps, J., Langille, M.G.I., Lee, J., Ley, R., Liu, Y.X., Loftfield, E., Lozupone, C., Maher, M., Marotz, C., Martin, B.D., McDonald, D., McIver, L.J., Melnik, A. V., Metcalf, J.L., Morgan, S.C., Morton, J.T., Naimey, A.T., Navas-Molina, J.A., Nothias, L.F., Orchanian, S.B., Pearson, T., Peoples, S.L., Petras, D., Preuss, M.L., Pruesse, E., Rasmussen, L.B., Rivers, A., Robeson, M.S., Rosenthal, P., Segata, N., Shaffer, M., Shiffer, A., Sinha, R., Song, S.J., Spear, J.R., Swafford, A.D., Thompson, L.R., Torres, P.J., Trinh, P., Tripathi, A., Turnbaugh, P.J., Ul-Hasan, S., van der Hooft, J.J.J., Vargas, F., Vázquez-Baeza, Y., Vogtmann, E., von Hippel, M., Walters, W., Wan, Y., Wang, M., Warren, J., Weber, K.C., Williamson, C.H.D., Willis, A.D., Xu, Z.Z., Zaneveld, J.R., Zhang, Y., Zhu, Q., Knight, R., Caporaso, J.G., 2019. Reproducible,

491 interactive, scalable and extensible microbiome data science using QIIME 2. Nat.
492 Biotechnol. 37, 852–857. https://doi.org/10.1038/s41587-019-0209-9
493 Callahan, B.J., McMurdie, P.J., Rosen, M.J., Han, A.W., Johnson, A.J.A., Holmes, S.P., 2016.
494 DADA2: High-resolution sample inference from Illumina amplicon data. Nat. Methods
495 13, 581–583. https://doi.org/10.1038/nmeth.3869
496 Capella-Gutiérrez, S., Silla-Martínez, J.M., Gabaldón, T., 2009. trimAl: A tool for automated
497 alignment trimming in large-scale phylogenetic analyses. Bioinformatics 25, 1972–1973.
498 https://doi.org/10.1093/bioinformatics/btp348
499 Chen, Yuxin, Chen, Yongsheng, Shi, C., Huang, Z., Zhang, Y., Li, S., Li, Y., Ye, J., Yu, C.,
500 Li, Z., Zhang, X., Wang, J., Yang, H., Fang, L., Chen, Q., 2018. SOAPnuke: A
501 MapReduce acceleration-supported software for integrated quality control and
502 preprocessing of high-throughput sequencing data. Gigascience 7, 1–6.
503 https://doi.org/10.1093/gigascience/gix120
504 Conthe, M., Wittorf, L., Kuenen, J.G., Kleerebezem, R., Van Loosdrecht, M.C.M., Hallin, S.,
505 2018. Life on N_2O: Deciphering the ecophysiology of N_2O respiring bacterial
506 communities in a continuous culture. ISME J. 12, 1142–1153.
507 https://doi.org/10.1038/s41396-018-0063-7

Dokoumetzidis, A., Macheras, P., 2006. A century of dissolution research: From Noyes and Whitney to the Biopharmaceutics Classification System. Int. J. Pharm. 321, 1–11. https://doi.org/10.1016/j.ijpharm.2006.07.011

Domingo-Félez, C., Smets, B.F., 2019. Regulation of key N_2O production mechanisms during biological water treatment. Curr. Opin. Biotechnol. 57, 119–126. https://doi.org/10.1016/j.copbio.2019.03.006

Duan, H., Zhao, Y., Koch, K., Wells, G.F., Zheng, M., Yuan, Z., Ye, L., 2021. Insights into Nitrous Oxide Mitigation Strategies in Wastewater Treatment and Challenges for Wider Implementation. Environ. Sci. Technol. 55, 7208–7224. https://doi.org/10.1021/acs.est.1c00840

Frutos, O.D., Quijano, G., Pérez, R., Muñoz, R., 2016. Simultaneous biological nitrous oxide abatement and wastewater treatment in a denitrifying off-gas bioscrubber. Chem. Eng. J. 288, 28–37. https://doi.org/10.1016/j.cej.2015.11.088

Hallin, S., Philippot, L., Löffler, F.E., Sanford, R.A., Jones, C.M., 2018. Genomics and Ecology of Novel N2O-Reducing Microorganisms. Trends Microbiol. 26, 43–55. https://doi.org/10.1016/j.tim.2017.07.003

Han, H., Kim, D.D., Song, M.J., Yun, T., Yoon, H., Lee, H.W., Kim, Y.M., Laureni, M., Yoon, S., 2023. Biotrickling Filtration for the Reduction of N_2O Emitted during

Wastewater Treatment: Results from a Long-Term In Situ Pilot-Scale Testing. Environ. Sci. Technol. 57, 3883–3892. https://doi.org/10.1021/acs.est.2c08818

Harris, E., Joss, A., Emmenegger, L., Kipf, M., Wolf, B., Mohn, J., Wunderlin, P., 2015. Isotopic evidence for nitrous oxide production pathways in a partial nitritation-anammox reactor. Water Res. 83, 258–270. https://doi.org/10.1016/j.watres.2015.06.040

Hu, Z., Zhang, J., Xie, H., Liang, S., Li, S., 2013. Minimization of nitrous oxide emission from anoxic-oxic biological nitrogen removal process: Effect of influent COD/NH_4^+ ratio and feeding strategy. J. Biosci. Bioeng. 115, 272–278. https://doi.org/10.1016/j.jbiosc.2012.09.016

Huang, K., He, Y., Wang, W., Jiang, R., Zhang, Y., Li, J., Zhang, X.X., Wang, D., 2024. Temporal differentiation in the adaptation of functional bacteria to low-temperature stress in partial denitrification and anammox system. Environ. Res. 244, 117933. https://doi.org/10.1016/j.envres.2023.117933

IPCC, 2022. Summary for Policymakers. In: Climate Change 2022: Mitigation of Climate Change, Cambridge University Press. https://doi.org/10.1017/9781009157926.001

Isokpehi, R.D., Kim, Y., Krejci, S.E., Trivedi, V.D., 2024. Ecological Trait-Based Digital Categorization of Microbial Genomes for Denitrification Potential. Microorganisms 12, 791. https://doi.org/10.3390/microorganisms12040791

544 Kalyaanamoorthy, S., Minh, B.Q., Wong, T.K.F., Von Haeseler, A., Jermiin, L.S., 2017.
545 ModelFinder: Fast model selection for accurate phylogenetic estimates. Nat. Methods 14,
546 587–589. https://doi.org/10.1038/nmeth.4285
547 Kampschreur, M.J., Temmink, H., Kleerebezem, R., Jetten, M.S.M., van Loosdrecht, M.C.M.,
548 2009. Nitrous oxide emission during wastewater treatment. Water Res. 43, 4093–4103.
549 https://doi.org/10.1016/j.watres.2009.03.001
550 Kampschreur, M.J., van der Star, W.R.L., Wielders, H.A., Mulder, J.W., Jetten, M.S.M., van
551 Loosdrecht, M.C.M., 2008. Dynamics of nitric oxide and nitrous oxide emission during
552 full-scale reject water treatment. Water Res. 42, 812–826.
553 https://doi.org/10.1016/j.watres.2007.08.022
554 Kartal, B., Kuypers, M.M.M., Lavik, G., Schalk, J., Op Den Camp, H.J.M., Jetten, M.S.M.,
555 Strous, M., 2007. Anammox bacteria disguised as denitrifiers: Nitrate reduction to
556 dinitrogen gas via nitrite and ammonium. Environ. Microbiol. 9, 635–642.
557 https://doi.org/10.1111/j.1462-2920.2006.01183.x
558 Katoh, K., Misawa, K., Kuma, K.I., Miyata, T., 2002. MAFFT: A novel method for rapid
559 multiple sequence alignment based on fast Fourier transform. Nucleic Acids Res. 30,
560 3059–3066. https://doi.org/10.1093/nar/gkf436
561 Kubota, K., Hayashi, M., Matsunaga, K., Iguchi, A., Ohashi, A., Li, Y.Y., Yamaguchi, T.,
562 Harada, H., 2014. Microbial community composition of a down-flow hanging sponge

(DHS) reactor combined with an up-flow anaerobic sludge blanket (UASB) reactor for the treatment of municipal sewage. Bioresour. Technol. 151, 144–150. https://doi.org/10.1016/j.biortech.2013.10.058

Kubota, K., Otani, T., Hariu, T., Jin, T., Tagawa, T., Morikawa, M., Li, Y.Y., 2024. Evaluation of sewage treatment performance and duckweed biomass production efficiency in a primary sedimentation basin + duckweed pond + downflow hanging sponge (PSB + DWP + DHS) system. J. Water Process Eng. 65, 105818. https://doi.org/10.1016/j.jwpe.2024.105818

Lackner, S., Gilbert, E.M., Vlaeminck, S.E., Joss, A., Horn, H., van Loosdrecht, M.C.M., 2014. Full-scale partial nitritation/anammox experiences – An application survey. Water Res. 55, 292–303. https://doi.org/10.1016/j.watres.2014.02.032

Letunic, I., Bork, P., 2021. Interactive tree of life (iTOL) v5: An online tool for phylogenetic tree display and annotation. Nucleic Acids Res. 49, W293–W296. https://doi.org/10.1093/nar/gkab301

Liu, P., Zou, S., Zhang, H., Liu, Q., Song, Z., Huang, Y., Hu, X., 2023. Genome-resolved metagenomics provides insights into the microbial-mediated sulfur and nitrogen cycling in temperate seagrass meadows. Front. Mar. Sci. 10, 1245288. https://doi.org/10.3389/fmars.2023.1245288

581 Matsubayashi, M., Shimada, Y., Li, Y.Y., Harada, H., Kubota, K., 2017. Phylogenetic
582 diversity and in situ detection of eukaryotes in anaerobic sludge digesters. PLoS One
583 12, e0172888. https://doi.org/10.1371/journal.pone.0172888
584 McDonald, D., Jiang, Y., Balaban, M., Cantrell, K., Zhu, Q., Gonzalez, A., Morton, J.T.,
585 Nicolaou, G., Parks, D.H., Karst, S.M., Albertsen, M., Hugenholtz, P., DeSantis, T.,
586 Song, S.J., Bartko, A., Havulinna, A.S., Jousilahti, P., Cheng, S., Inouye, M., Niiranen,
587 T., Jain, M., Salomaa, V., Lahti, L., Mirarab, S., Knight, R., 2023. Greengenes2 unifies
588 microbial data in a single reference tree. Nat. Biotechnol. 42, 715–718.
589 https://doi.org/10.1038/s41587-023-01845-1
590 Minh, B.Q., Schmidt, H.A., Chernomor, O., Schrempf, D., Woodhams, M.D., Von Haeseler,
591 A., Lanfear, R., Teeling, E., 2020. IQ-TREE 2: New Models and Efficient Methods for
592 Phylogenetic Inference in the Genomic Era. Mol. Biol. Evol. 37, 1530–1534.
593 https://doi.org/10.1093/molbev/msaa015
594 Newell, R.J.P., Aroney, S.T.N., Zaugg, J., Sternes, P., Tyson, G.W., Woodcroft, B.J., 2023.
595 Aviary : Hybrid assembly and genome recovery from metagenomes with Aviary (v0.8.3).
596 Zenodo. https://doi.org/10.5281/zenodo.10158086.
597 Ni, J., Hatori, S., Wang, Y., Li, Y.Y., Kubota, K., 2020. Uncovering Viable Microbiome in
598 Anaerobic Sludge Digesters by Propidium Monoazide (PMA)-PCR. Microb. Ecol. 79,
599 925–932. https://doi.org/10.1007/s00248-019-01449-w

Noyes, A.A., Whitney, W.R., 1897. The rate of solution of solid substances in their own solutions. J. Am. Chem. Soc. 19, 930–934.

Oba, K., Suenaga, T., Yasuda, S., Kuroiwa, M., Hori, T., Lackner, S., Terada, A., 2024. Quest for Nitrous Oxide-reducing Bacteria Present in an Anammox Biofilm Fed with Nitrous Oxide. Microbes Environ. 39, ME23106. https://doi.org/10.1264/jsme2.ME23106

Okabe, S., Oshiki, M., Takahashi, Y., Satoh, H., 2011. N_2O emission from a partial nitrification-anammox process and identification of a key biological process of N2O emission from anammox granules. Water Res. 45, 6461–6470. https://doi.org/10.1016/j.watres.2011.09.040

Peng, L., Carvajal-Arroyo, J.M., Seuntjens, D., Prat, D., Colica, G., Pintucci, C., Vlaeminck, S.E., 2017. Smart operation of nitritation/denitritation virtually abolishes nitrous oxide emission during treatment of co-digested pig slurry centrate. Water Res. 127, 1–10. https://doi.org/10.1016/j.watres.2017.09.049

Qi, C., Zhou, Y., Suenaga, T., Oba, K., Lu, J., Wang, G., Zhang, L., Yoon, S., Terada, A., 2022. Organic carbon determines nitrous oxide consumption activity of clade I and II nosZ bacteria: Genomic and biokinetic insights. Water Res. 209, 117910. https://doi.org/10.1016/j.watres.2021.117910

617 Quan, Z.X., Im, W.T., Lee, S.T., 2006. *Azonexus caeni* sp. nov., a denitrifying bacterium
618 isolated from sludge of a wastewater treatment plant. Int. J. Syst. Evol. Microbiol. 56,
619 1043–1046. https://doi.org/10.1099/ijs.0.64019-0
620 Ramírez-Fernández, L., Orellana, L.H., Johnston, E.R., Konstantinidis, K.T., Orlando, J.,
621 2021. Diversity of microbial communities and genes involved in nitrous oxide emissions
622 in Antarctic soils impacted by marine animals as revealed by metagenomics and 100
623 metagenome-assembled genomes. Sci. Total Environ. 788, 147693.
624 https://doi.org/10.1016/j.scitotenv.2021.147693
625 Ravishankara, A.R., Daniel, J.S., Portmann, R.W., 2009. Nitrous oxide (N_2O): The dominant
626 ozone-depleting substance emitted in the 21st century. Science 326, 123–125.
627 https://doi.org/10.1126/science.1176985
628 Rognes, T., Flouri, T., Nichols, B., Quince, C., Mahé, F., 2016. VSEARCH: A versatile open
629 source tool for metagenomics. PeerJ 4, e2584. https://doi.org/10.7717/peerj.2584
630 Sabba, F., Terada, A., Wells, G., Smets, B.F., Nerenberg, R., 2018. Nitrous oxide emissions
631 from biofilm processes for wastewater treatment. Appl. Microbiol. Biotechnol. 102,
632 9815–9829. https://doi.org/10.1007/s00253-018-9332-7
633 Seemann, T., 2014. Prokka: Rapid prokaryotic genome annotation. Bioinformatics 30,
634 2068–2069. https://doi.org/10.1093/bioinformatics/btu153

Suenaga, T., Riya, S., Hosomi, M., Terada, A., 2018. Biokinetic characterization and activities of N_2O-reducing bacteria in response to various oxygen levels. Front. Microbiol. 9, 697. https://doi.org/10.3389/fmicb.2018.00697

Tanikawa, D., Motokawa, D., Itoiri, Y., Kimura, Z.I., Ito, M., Nagano, A., 2022. Biogas purification and ammonia load reduction in sewage treatment by two-stage down-flow hanging sponge reactor. Sci. Total Environ. 851, 158355. https://doi.org/10.1016/j.scitotenv.2022.158355

Tian, H., Xu, R., Canadell, J.G., Thompson, R.L., Winiwarter, W., Suntharalingam, P., Davidson, E.A., Ciais, P., Jackson, R.B., Janssens-Maenhout, G., Prather, M.J., Regnier, P., Pan, N., Pan, S., Peters, G.P., Shi, H., Tubiello, F.N., Zaehle, S., Zhou, F., Arneth, A., Battaglia, G., Berthet, S., Bopp, L., Bouwman, A.F., Buitenhuis, E.T., Chang, J., Chipperfield, M.P., Dangal, S.R.S., Dlugokencky, E., Elkins, J.W., Eyre, B.D., Fu, B., Hall, B., Ito, A., Joos, F., Krummel, P.B., Landolfi, A., Laruelle, G.G., Lauerwald, R., Li, W., Lienert, S., Maavara, T., MacLeod, M., Millet, D.B., Olin, S., Patra, P.K., Prinn, R.G., Raymond, P.A., Ruiz, D.J., van der Werf, G.R., Vuichard, N., Wang, J., Weiss, R.F., Wells, K.C., Wilson, C., Yang, J., Yao, Y., 2020. A comprehensive quantification of global nitrous oxide sources and sinks. Nature 586, 248–256. https://doi.org/10.1038/s41586-020-2780-0

Vasilaki, V., Massara, T.M., Stanchev, P., Fatone, F., Katsou, E., 2019. A decade of nitrous oxide (N_2O) monitoring in full-scale wastewater treatment processes: A critical review. Water Res. 161, 392–412. https://doi.org/10.1016/j.watres.2019.04.022

Wang, S., Yuan, C., Xu, C., Li, D., Zhang, H., Wang, J., Wang, X., Li, Y., Jiao, D., Yuan, S., Chen, H., Qiu, D., 2024. Denitrificimonas halotolerans sp. nov., a novel species isolated from UASB sludge treating landfill leachate. Antonie van Leeuwenhoek, Int. J. Gen. Mol. Microbiol. 117, 91. https://doi.org/10.1007/s10482-024-01987-5

Wang, X., Xiang, B., Li, J., Zhang, M., Frostegard, A., Bakken, L., Zhang, X., 2023. Using adaptive and aggressive N_2O-reducing bacteria to augment digestate fertilizer for mitigating N_2O emissions from agricultural soils. Sci. Total Environ. 903, 166284. https://doi.org/10.1016/j.scitotenv.2023.166284

Watanabe, T., Kojima, H., Umezawa, K., Hori, C., Takasuka, T.E., Kato, Y., Fukui, M., 2019. Genomes of neutrophilic sulfur-oxidizing chemolithoautotrophs representing 9 proteobacterial species from 8 genera. Front. Microbiol. 10, 00316. https://doi.org/10.3389/fmicb.2019.00316

Wu, L., Peng, L., Wei, W., Wang, D., Ni, B.J., 2020. Nitrous oxide production from wastewater treatment: The potential as energy resource rather than potent greenhouse gas. J. Hazard. Mater. 387, 121694. https://doi.org/10.1016/j.jhazmat.2019.121694

Yamaguchi, Tsuyoshi, Nakamura, S., Hatamoto, M., Tamura, E., Tanikawa, D., Kawakami, S., Nakamura, A., Kato, K., Nagano, A., Yamaguchi, Takashi, 2018. A novel approach for toluene gas treatment using a downflow hanging sponge reactor. Appl. Microbiol. Biotechnol. 102, 5625–5634. https://doi.org/10.1007/s00253-018-8933-5

Yoon, H., Song, M.J., Kim, D.D., Sabba, F., Yoon, S., 2019. A Serial Biofiltration System for Effective Removal of Low-Concentration Nitrous Oxide in Oxic Gas Streams: Mathematical Modeling of Reactor Performance and Experimental Validation. Environ. Sci. Technol. 53, 2063–2074. https://doi.org/10.1021/acs.est.8b05924

Yoon, H., Song, M.J., Yoon, S., 2017. Design and Feasibility Analysis of a Self-Sustaining Bio fi ltration System for Removal of Low Concentration N2O Emitted from Wastewater Treatment Plants. https://doi.org/10.1021/acs.est.7b02750

Yoon, S., Nissen, S., Park, D., Sanford, R.A., Löffler, E., 2016. Clade I NosZ from Those Harboring Clade II NosZ. Appl. Envioronmental Microbiol. 82, 3793–3800. https://doi.org/10.1128/AEM.00409-16.Editor

Zhang, Z., Zhang, Y., Shi, Z., Chen, Y., 2022. Linking Genome-Centric Metagenomics to Kinetic Analysis Reveals the Regulation Mechanism of Hydroxylamine in Nitrite Accumulation of Biological Denitrification. Environ. Sci. Technol. 56, 10317–10328. https://doi.org/10.1021/acs.est.2c01914

Zheng, X., Yan, Z., Zhao, C., He, L., Lin, Z., Liu, M., 2023. Homogeneous environmental selection mainly determines the denitrifying bacterial community in intensive aquaculture water. Front. Microbiol. 14, 1280450. https://doi.org/10.3389/fmicb.2023.1280450